AIP Conference Proceedings

RESEARCH ARTICLE | JUNE 27 2023

Electrical properties and microstructure of crystalline silicon ingots grown from quartz crucibles with and without diffusion barriers

Rune Søndenå ✉; Gaute Stokkan; Jochen Busam; Rania Hendawi; Benny Hallam; Marisa Di Sabatino

AIP Conf. Proc. 2826, 110009 (2023)
https://doi.org/10.1063/5.0141154

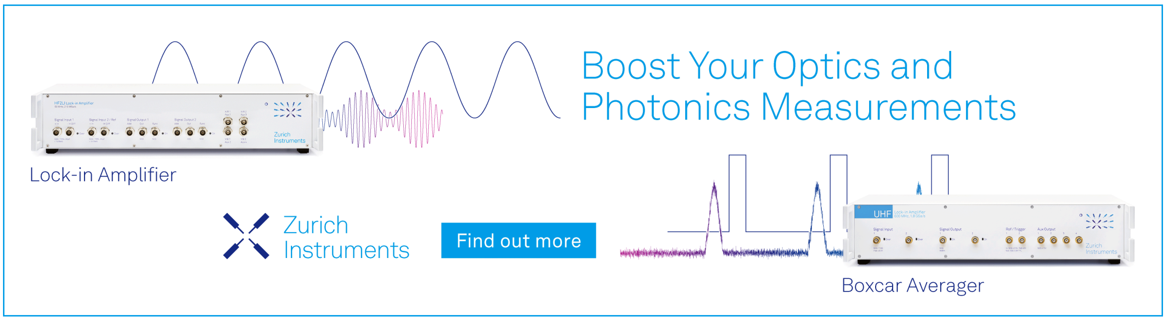

AIP Publishing

Electrical Properties and Microstructure of Crystalline Silicon Ingots Grown From Quartz Crucibles With and Without Diffusion Barriers

Rune Søndenå[1, a)], Gaute Stokkan[2], Jochen Busam[3], Rania Hendawi[3], Benny Hallam[4], and Marisa Di Sabatino[3]

[1]*Institute for Energy Technology, 2007 Kjeller, Norway*
[2]*SINTEF Industry, 7461 Trondheim, Norway*
[3]*NTNU, Department of Materials Science and Engineering, 7491 Trondheim, Norway*
[4]*The Quartz Corp., 8270 Drag, Norway*

[a)] Corresponding author: rune.sondena@ife.no

Abstract. Three hybrid ingots, where half the seed area was filled with fluidized bed reactor granules for high-performance multicrystalline silicon growth and the other half with monocrystalline slabs for mono-like growth, were made. The ingots were solidified in quartz crucibles with two different diffusion barriers and one reference crucible with no diffusion barrier. The material quality of these three ingots was compared with respect to minority carrier lifetime and crystal structure. High purity silica was used in one diffusion barrier, while a fraction of high purity quartz sand was mixed with such silica in the second diffusion layer. High purity quartz sand was mixed in to further increase the purity of the diffusion barrier, thus, reduce the low lifetime regions (or red-zones). The results indicate that the diffusion barriers between the quartz crucible and the directionally solidified silicon ingots reduce the extent of the red-zones, which implies that diffusion barriers aid in decreasing the amount of metallic impurities (particularly Fe) implemented into the silicon ingot. No visible changes to the crystal structure were observed between the two ingots with diffusion barrier.

INTRODUCTION

Due to the high melting temperature (1412 °C) and reactivity of silicon at such temperatures, not many materials are suitable for melting and solidification of silicon. Thus, crucibles for silicon photovoltaic and electronic applications are made from silicon dioxide in the form of amorphous quartz, also called amorphous silica. Provided a high enough quartz purity, in the case of reaction or dissolution only silicon and oxygen are released into the silicon melt. In the production of silicon ingots by directional solidification an inexpensive and comparably impurity-rich slip-cast amorphous silica crucible is used and coated by silicon nitride to prevent reaction with the melt. Potential impurities in the feedstock, crucibles, coatings, and ingots have previously been evaluated for multicrystalline silicon solar cells produced by directional solidification[1]. The crucible has been found to be the main source for performance-limiting impurities, with potential contributions also from the nitride coating and the feedstock. Low minority carrier lifetime areas in the ingots near the crucible walls caused by in-diffused metallic impurities are called red-zones[2]. A layer of high purity (HP) quartz in addition to the nitride coating between the crucible and the melt can improve the diffusion barrier for metal impurities, reducing the potential contamination of the silicon melt from the less pure outer layer of the quartz crucible[3]. Former investigations of different commercial SiO_2 diffusion layers showed a positive impact on the lifetime of multicrystalline Si ingots[4]. The performance of the barrier is highly influenced by its porosity, thickness, and purity[4]. In the present work, the effect of high-purity (HP) diffusion barriers on the electrical and microstructural properties of crystalline silicon ingots cast using directional solidification has been investigated for multicrystalline (mc) and mono-like silicon ingots. Two ingots are made using diffusion barriers with different compositions, and one ingot is made in a standard quartz crucible without a diffusion barrier.

SiliconPV 2022, the 12th International Conference on Crystalline Silicon Photovoltaics
AIP Conf. Proc. 2826, 110009-1–110009-5; https://doi.org/10.1063/5.0141154
Published by AIP Publishing. 978-0-7354-4536-9/$30.00

EXPERIMENTAL DETAILS

Three p-type (B-doped) hybrid ingots[5], where half the bottom is seeded with fluidized bed reactor (FBR) granules and the other half is seeded with slabs cut from a Czochralski (Cz) ingot, were grown in a Crystalox DS 250 directional solidification furnace according to the same procedures followed in previous studies[6]–[8]. The ingots were made in slip-cast fused quartz crucibles with different diffusion layers:

1. A reference ingot with no additional diffusion barrier (*Reference ingot*)
2. A high-purity (HP) silica diffusion barrier *(HP-silica barrier ingot)*
3. A diffusion barrier consisting of a mix of HP silica and natural HP quartz sand *(silica/sand barrier ingot)*

A thin layer of silicon nitride coating, which is composed of 90% α-Si_3N_4 was applied on the inner surface of the crucibles to prevent silicon sticking and facilitate the ingot removal. Casting conditions and parameters were similar for all the ingots. 0.5 mm thick wafers (cut perpendicularly to the growth direction) were then made from the center of each ingot, while 2 mm thick vertical cross sections (parallel to the growth direction) were cut from the sides closer to the outer perimeter of each ingot. The cross sections for each ingot were polished and etched isotropically using an HNA-solution, as described in in Ref.[9]. Optical images at different angles of incidence reveal the dislocations in the etched samples. Wafers from three heights were selected from each ingot, polished, and etched. Furthermore, Laue scanning was used to obtain the grain orientation mapping of the cross sections. Minority carrier lifetime maps were carried out by micro-wave photoconductance decay (micro-PCD) on non-passivated side-cuts, and photoluminescence (PL) imaging of surface passivated wafers. Processing of the wafers include damage etching followed by an emitter in-diffusion in a $POCl_3$ tube-furnace[10]. After plasma enhanced chemical vapor deposition (PECVD) of a hydrogen rich SiN_X anti-reflection coating (ARC) on both sides, the wafers were exposed to a simulated contact firing step[11], [12]. After an etch-back of the ARC and the emitter the wafers were passivated using PECVD deposited amorphous silicon on both sides. Minority carrier lifetimes are then measured using QssPC (Sinton WCT-120TS).

RESULTS AND DISCUSSION

Lifetime maps of vertical side-cuts from the three ingots are shown in Figures 1 a) to c). Multicrystalline and mono-like regions are shown on the left- and the right-hand-side of each cross-section, respectively. It is possible to distinguish the mono-like areas from the multicrystalline areas by the absence of grain boundaries. However, some dislocation growth can still be seen in the mono-like areas. The extent of the low lifetime red-zone in the side-cuts, with high levels of metal impurities, is reduced in both ingots cast with a diffusion barrier. With the high purity silica diffusion barrier, the lateral extent of the red-zone was reduced by 40% relative to the reference ingot. However, the barrier with an addition of high purity quartz sand, showed a 45% decrease in the lateral red zone thickness. No significant differences between the multicrystalline and the monocrystalline regions can be seen with respect to the red-zone from the crucible walls. However, dislocations in the mono-like region of the HP silica barrier ingot seem to increase the extent of the low lifetime region near the crucible bottom in Figure 2b). This may also be a result of insufficient gettering of metallic impurities, as the gettering efficacy in grain boundary and dislocation rich areas, often decorated with impurities, is limited[13].

Figure 1 d) shows a photoluminescence image of a gettered and hydrogenated wafer from approximately 64% height in Ingot 1. Figure 1d) clearly shows the mono-like and multicrystalline regions on the top and bottom parts of the wafer, respectively. The average lifetimes, chosen from smaller areas within each region, are shown for all three ingots in Figure 2. After gettering and hydrogenation higher lifetimes were measured in wafers from the silica/sand barrier ingot than in wafers from the HP silica barrier ingot in the mono-like areas, with an exception in the highest position. Wafers from the top position of the silica/sand barrier ingot are, however, strongly affected by dislocations in the mono-like areas. In the multi-crystalline areas, the lifetimes in wafers from the silica/sand barrier ingot are higher than in the HP silica barrier ingot for all wafer heights.

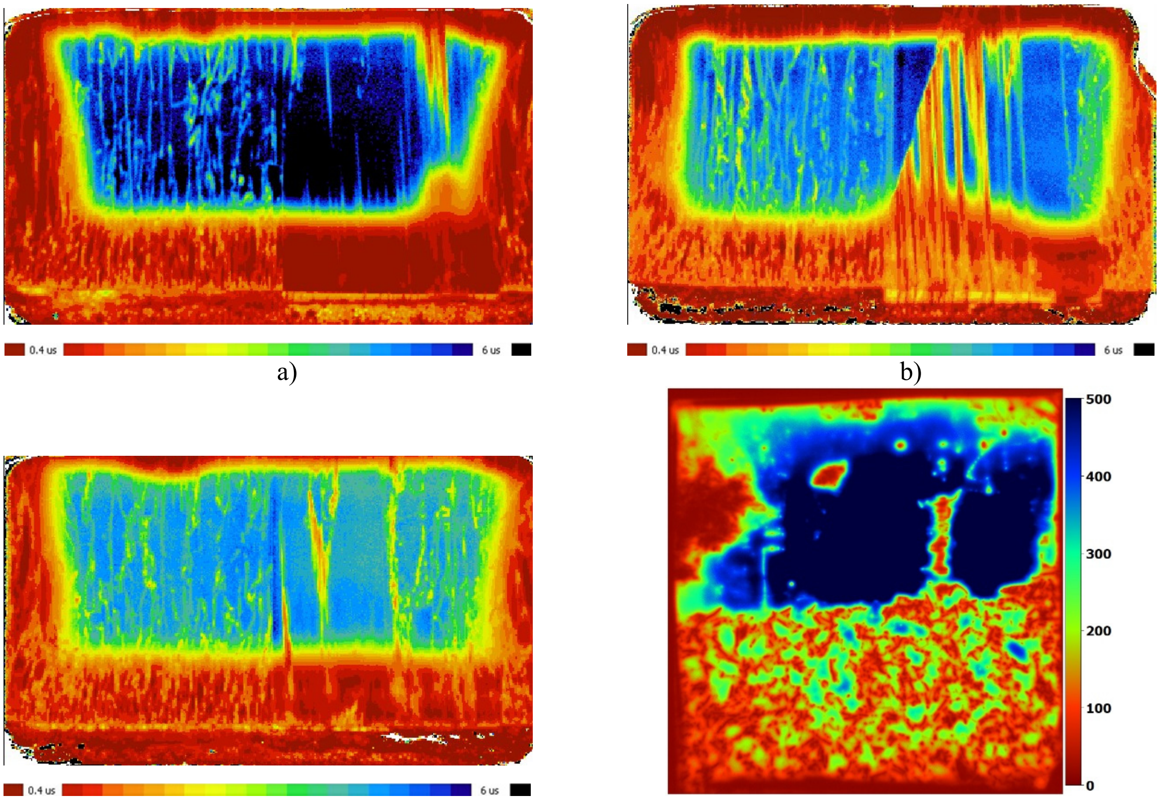

a) b) c) d)

FIGURE 1 Minority carrier lifetime maps by micro-PCD for non-passivated vertical side-cuts from a) the reference ingot, b) the HP silica barrier ingot, and c) the ingot with a HP silica and HP quartz sand barrier. A PL-image of a wafer from ca. 64% height in the reference ingot is shown in d). The scales are in microseconds.

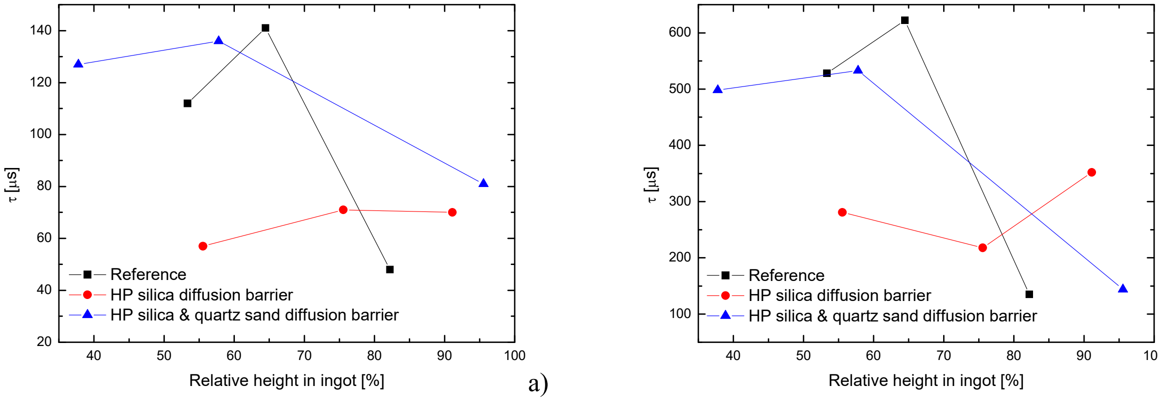

a) b)

FIGURE 2 Average lifetimes in phosphorus diffusion gettered and hydrogenated wafers for a) the mc-Si areas, and b) the mono-like areas for different heights in the ingots.

The dislocation mapping of the silica/sand barrier ingot cross-sections showed higher dislocation density in the mono-like area compared to the other two ingots which might explain the low lifetime values towards the top of the silica/sand ingot. An opposite trend, with decreasing dislocation density towards the top, is noticed in the HP silica barrier ingot, which may explain the increase in the lifetime of towards the top in the mono-like region. Figures 3 and 4 show the Orientation Image Micrographs (OIM) of the ingots by Laue scan with the respective inverse pole figure (IPF). The fraction of random grain boundaries of the HP silica barrier ingot decreases by 2% from about 47% to 88% of the ingot height. Comparable fractions of Σ27 and random GB are found for all three ingots.

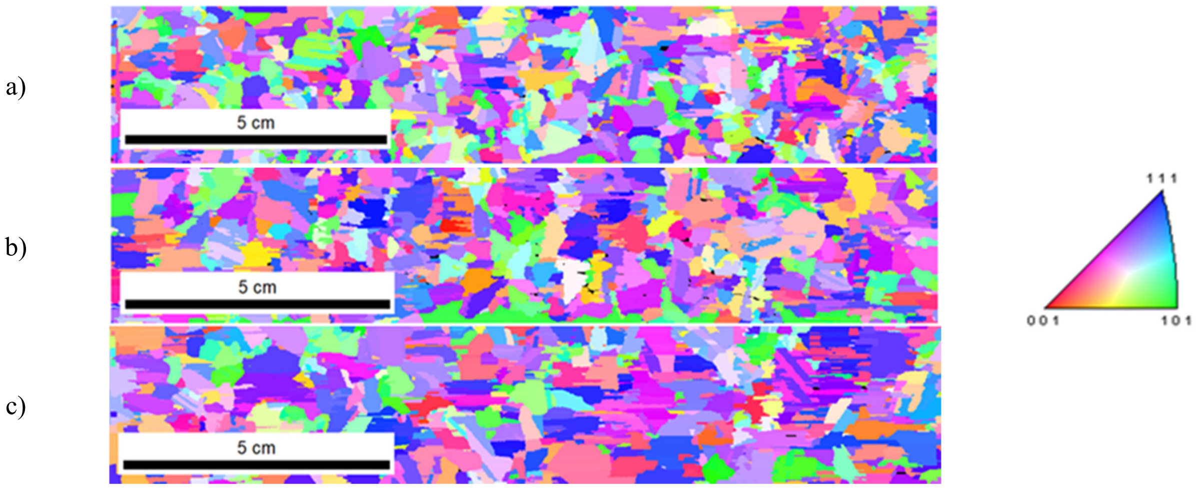

FIGURE 3 OIM's for the mc-Si areas of the Ingot 2 obtained by Laue X-ray for horizontal slabs at three relative heights (a-c): 47%, 68% and 88%, respectively. The IPF color legend map is shown on the right.

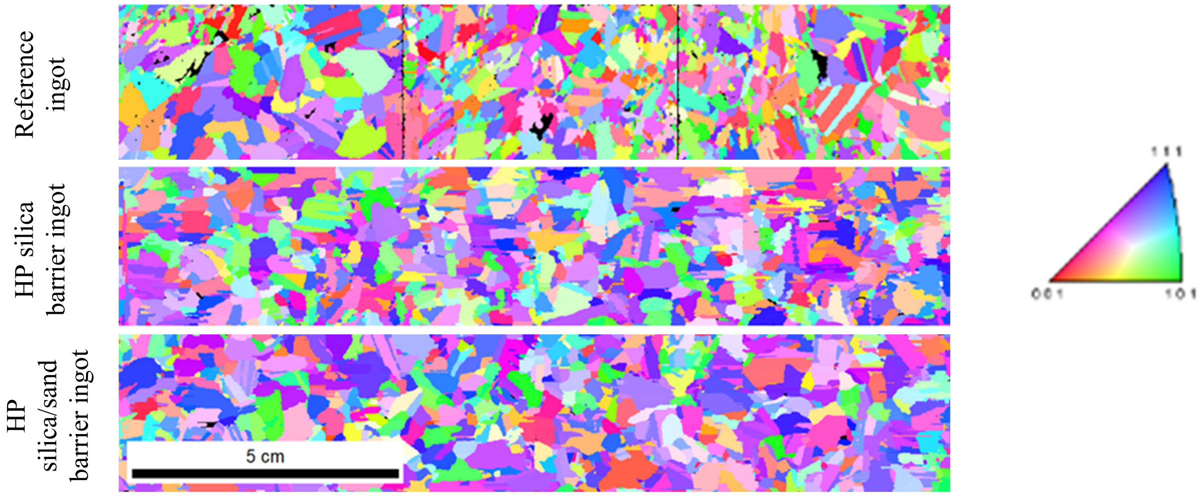

FIGURE 4 OIM's for the multi-crystalline areas of all three ingots. The horizontal slabs are at 45% height of the ingots.

As expected, the presence of a diffusion barrier in the crucible does not affect the microstructure and grain orientation of the ingot, while there is a clear effect on the impurity distribution (mainly proven by the lifetime maps) and dislocation density (due again to the presence of metallic impurities). Quantitative impurity distributions both in the crucibles and ingots investigated in this work will be presented in a future publication and seem to support these conclusions.

SUMMARY

In this work, the effect of the crucible material on the silicon ingot properties is investigated. Samples from hybrid silicon ingots partly seeded with FBR granules for high performance multicrystalline growth and partly with monocrystalline slabs for mono-like growth are studied in terms of the minority carrier lifetimes and the microstructure. Three such ingots have been grown: a reference ingot without a diffusion barrier, an ingot with a HP silica barrier, and an ingot with a diffusion barrier made of a mix of HP silica and HP quartz sand. Lifetime maps on non-passivated vertical side-cuts indicate that the presence of a diffusion barrier will reduce the extent of the in-diffusion of metallic elements from the crucible during solidification relative to the reference ingot without a barrier. A fraction of high purity quartz sand can be added to the diffusion barrier for improved minority carrier lifetimes.

However, dislocations may still affect the measured lifetimes in passivated wafers, especially in the mono-like regions. The grain orientation maps by Laue scan do not reveal any significant differences among the three ingots.

ACKNOWLEDGMENTS

This work was funded by the Norwegian Research Council and industrial partners through the project *Crucibles for Next Generation High-Quality Silicon Solar Cells* (#268027).

REFERENCES

1. Stokkan, G., *et al.*, "Impurity control in high performance multicrystalline silicon," *Phys. Status Solidi A Appl. Mater. Sci.*, 214, 1700319, 2017.
2. Boulfrad, Y., *et al.*, "Modeling of Lifetime Distribution in a Multicrystalline Silicon Ingot," *Solid State Phenom.*, 178–179, 507–512, 2011.
3. Laurent, J., *et al.*, "Crucible Contribution to Cell Efficiency and Process Yield," in *31st EU PVSEC*, Hamburg, Germany, 2015.
4. Trempa, M. *et al.*, "Impact of different SiO_2 diffusion barrier layers on lifetime distribution in multi-crystalline silicon ingots," *J. Crystal Growth*, 532, 125378, 2020.
5. Adamczyk, K., *et al.*, "Recombination Strength of Dislocations in High-Performance Multicrystalline/Quasi-Mono Hybrid Wafers During Solar Cell Processing," *Phys. Status Solidi A Appl. Mater. Sci.*, 215, 1700493, 2017.
6. Adamczyk, K., *et al.*, "Recombination activity of grain boundaries in high-performance multicrystalline Si during solar cell processing," *J. Appl. Phys.*, 123, 55705, 2018.
7. Ekstrøm, K.-E., *et al.*, "Microstructure of multicrystalline silicon seeded by polysilicon chips and fluidized bed reactor granules," *J.Crystal Growth*, 441, 95–100, 2016.
8. Ekstrøm, K.-E., *et al.*, "Structure and dislocation development in mono-like silicon," *Phys. Status Solidi A Appl. Mater. Sci.*, 212, 2278-2288, 2015.
9. Adamczyk, K., *et al.*, "Guidelines for establishing an etching procedure for dislocation density measurements on multicrystalline silicon samples," *MethodsX*, 5, 1178–1186, 2018.
10. Syre, M., *et al.*, "Evaluation of possible mechanisms behind P gettering of iron," *J. Appl. Phys.*, 110, 24912, 2011.
11. Søndenå, R., *et al.*, "Evolution of defect densities with height in a HPMC-Si ingot," *AIP Conf. Proc.*, 2147, 140010, 2019, https://aip.scitation.org/doi/abs/10.1063/1.5123897.
12. Søndenå, R., Wiig, M. S., "Evolution of the light sensitive defects in high performance multicrystalline silicon wafers," *J. Appl. Phys.*, 125, 85701, 2019.
13. Bentzen, A. *et al.*, "Gettering of transition metal impurities during phosphorus emitter diffusion in multicrystalline silicon solar cell processing," *J. Appl. Phys.*, 99, 093509, 2006.